

# Diffusion tensor imaging and diffusion-weighted imaging on axillary lymph node status in breast cancer patients

Nazmi Kurt   
Busem Binboga Kurt   
Ugur Gulsaran   
Burak Uslu   
Ahmet Onur Celik   
Necdet Sut   
Ebru Tastekin   
Derya Karabulut   
Nermin Tuncbilek 

## PURPOSE

This article will examine the usefulness of diffusion tensor imaging (DTI) and diffusion-weighted imaging (DWI) on the assessment of axillary lymph nodes (ALN) of breast cancer patients.

## METHODS

Axillary lymph nodes in 66 breast cancer patients were examined by DTI and DWI, and the largest lymph node with increased cortical thickness in axilla was selected. Morphological features, apparent diffusion coefficient (ADC), volume anisotropy, and fractional anisotropy values were measured by using a special software. Imaging findings and histopathological results were recorded.

## RESULTS

Metastatic ALN were detected in 43 (65.1%) patients. Cortical thickness of the metastatic ALN was significantly higher than the non-metastatic ALNs ( $P < .001$ ), and the long-axis-to-short-axis ratio was significantly lower in metastatic ALNs ( $P < .001$ ). There was a statistically significant difference between the ALN status and fatty hilum presence ( $P < .001$ ). Apparent diffusion coefficient values of metastatic ALNs were statistically lower than those of non-metastatic ALNs ( $P < .001$ ) using a cutoff value of  $1.26 \times 10^{-3} \text{ mm}^2/\text{s}$  for  $b=500$  ADC and  $1.21 \times 10^{-3} \text{ mm}^2/\text{s}$  for  $b=800$  ADC which had 97.7% sensitivity and 91.3% specificity. Fractional anisotropy and volume anisotropy values were significantly different between both groups. A cutoff value of 0.47 for  $b=500$  fractional anisotropy had 83.7% sensitivity, 69.6% specificity 69.6% positive predictive value, and 83.7% negative predictive value. A cutoff value of 0.33 for  $b=500$  volume anisotropy had 76.7% sensitivity, 78.3% specificity, 86.8% positive predictive value, and 64.3% negative predictive value.

## CONCLUSION

Apparent diffusion coefficient value of metastatic ALNs was found to be significantly lower than those of non-metastatic ALN, and DTI metrics of metastatic ALN were found to be significantly higher than those of non-metastatic ALN. Overall, ADC had a better diagnostic performance than morphological features, fractional anisotropy, and volume anisotropy. Diffusion tensor imaging-derived diffusion metrics may be used to complement breast magnetic resonance imaging in the future after further standardization of the imaging parameters.

Preoperative staging is the most important step of clinical management and prediction in breast cancer.<sup>1</sup> Axillary lymph nodes (ALN) involvement has significant importance in these terms. Therefore, preoperative ALN evaluation has become one of the most important parameters in the surgical decision of axillary dissection in addition to breast-sparing surgery or radical mastectomy.<sup>2</sup>

Preoperative imaging of the axilla is very important to detect the presence of metastatic disease in non-palpable ALN. Although mammography is the standard imaging method in breast diseases, it is not considered reliable for imaging the axilla due to limited visualization of the axillary region.<sup>3</sup> Ultrasound (US) is the initial method of choice for evaluating ALN involvement in breast cancer patients, but with variable sensitivity and specificity.<sup>4,5</sup> However, US efficiency is limited in non-palpable lymph nodes and US evaluation depends on the daily routine of the radiologist.<sup>6</sup> Ultrasound-guided lymph node sampling, such as fine-needle aspiration and core-needle biopsy, can provide a clear diagnosis to confirm the

From the Departments of Radiology (N.K. ✉ nazmikurtx@gmail.com, U.G., B.U., A.O.C., D.K., N.T.), Pathology (B.B.K., E.T.), and Biostatistics (N.S.), Trakya University School of Medicine, Edirne, Turkey.

Received 2 May 2021; revision requested 24 May 2021; last revision received 24 October 2021; accepted 27 December 2021.

Available online: 18 May 2022.

DOI: 10.5152/dir.2022.21460

You may cite this article as: Kurt N, Kurt BB, Gulsaran U, et al. Diffusion tensor imaging and diffusion-weighted imaging on axillary lymph node status in breast cancer patients. *Diagn Interv Radiol.* 2022;28(4):329-336.

presence of metastasis in a suspicious node on imaging, but these are invasive methods and require an experienced pathologist.<sup>4,5</sup>

Dynamic contrast-enhanced magnetic resonance imaging (DCE-MRI) is an important tool to detect breast cancer and metastatic ALN with high sensitivity. However, due to lower specificity, additional supportive tools may be required to differentiate benign lesions from malignancy.<sup>7</sup> Moreover, in some cases, it is difficult to obtain clear results in breast MRI examination because contrast material cannot be administered to patients for various reasons, like an allergy.<sup>8</sup> Therefore, MRI sequences such as diffusion tensor imaging (DTI) and diffusion-weighted imaging (DWI) are increasingly important as they enable us to detect cellular environmental changes.<sup>9,10</sup>

Recent studies showed the importance of DWI in detecting ALN metastasis in breast cancer and the apparent diffusion coefficient (ADC) value has been found to be significantly lower in metastatic lymph nodes.<sup>11-13</sup> Diffusion tensor imaging, a more specific variant of DWI, can detect the degree of diffusion in at least 6 directions using additional gradients and provide more information about the microstructure. Fractional anisotropy (FA) and volume anisotropy (VA) provide quantitative analysis of anisotropic water diffusion in the tissue.<sup>14,15</sup> Diffusion tensor imaging has been used in limited studies to differentiate breast lesions, and variable FA values have been obtained.<sup>14,16,17</sup> This is the only detailed study that evaluates DTI metrics for the ALN status in breast cancer patients in the English literature.

Due to the importance of ALN status in preoperative setting to avoid unnecessary lymph node dissection, further imaging techniques are required to define optimal

results for all patients. In order to contribute, we aimed to evaluate FA, VA, and ADC values obtained from DTI and DWI in determining the ALN status in breast cancer.

## Methods

In this retrospective research, informed consent was obtained from the patients participating in the study, and approval was given by the Scientific Research Ethics Committee of Trakya University Medical Faculty (2019/31).

Sixty-six patients who had been diagnosed with breast cancer between May 2016 and July 2019 and underwent DTI in addition to preoperative DWI and DCE-MRI in our center were included in the study. Positive lymph nodes were determined by sentinel lymph node sampling and/or axillary dissection. When several metastatic lymph nodes were detected in axillary dissection, the largest lymph node size was reported by pathologists and this lymph node was evaluated by imaging techniques. Cases for which sentinel lymph node sampling resulted as tumor negative were accepted as non-metastatic lymph nodes.

Patients who did not give consent, who were not able to have an MRI examination (e.g., claustrophobia or MRI incompatible implant), who had a history of breast surgery or received neoadjuvant chemotherapy for breast cancer, and who had images with poor diagnostic quality (e.g., due to artifacts or distortions) were excluded from the study.

### Image analysis

Breast MRI was performed with a 1.5 Tesla scanner (Signa HDxt Excite II, GE Healthcare) and with a dedicated 7-channel coil on patients in the prone position. The time required to obtain the DTI sequence ranged from 10 to 15 minutes in addition to routine breast MRI. Short-time inversion

recovery (STIR) images, turbo spin-echo T2-weighted images, single-shot echo-planar images, and dynamic pre-contrast and post-contrast fat-suppressed images were obtained. The T2-weighted axial spin-echo sequence was obtained with the following parameters: repetition time (TR)=4700 ms, echo time (TE)=90 ms, field of view (FOV)=360, and slice thickness=3 mm. Then, axial STIR was obtained with the following parameters: TR=4700 ms, TE=90 ms, FOV=360, and slice thickness=3 mm.

Morphologically, the long axis, long-axis-to-short-axis ratio, cortical thickness, and the presence of a fatty hilum of the ALN were noted. Similar to many studies, we evaluated the largest lymph node with increased cortex thickness and obliterated hilum in our study.<sup>18,19</sup> All data were compared with perioperative sentinel lymph node sampling and axillary dissection results.

Diffusion gradients were applied in 6 directions for DTI, and FA and VA values from DTI were measured with b values of 200 and 500 s/mm<sup>2</sup>. Diffusion-weighted imaging and DTI were obtained with the following parameters: TR=5000 ms, TE=90 ms, slice thickness=3.0 mm, interslice gap=1, and FOV=360 mm. The apparent diffusion coefficient, FA, and VA value maps were created automatically by the imaging console for the quantitative analysis. Apparent diffusion coefficient values were measured separately with b values of 0, 500, and 800 s/mm<sup>2</sup>.

Diffusion-weighted imaging and DTI parameters were calculated by selecting the largest lymph node on the ADC, FA, and VA map, placing 3 regions of interest (ROI) in the cortex of the selected lymph node and calculating the mean. Three ROIs were attentively placed on the cortex. Necrotic and cystic components as well as axillary fat or hilum were excluded. The ROI area in the selected axillary lymph nodes was between 27 and 32 mm<sup>2</sup> (fixed 16 pixels).

### Main points

- Metastatic axillary lymph nodes (ALN) showed significantly higher fractional anisotropy (FA) values and lower apparent diffusion coefficient values.
- Apparent diffusion coefficient value has higher specificity and sensitivity compared to FA value in detecting metastatic lymph nodes.
- Diffusion-weighted imaging and diffusion tensor imaging magnetic resonance imaging metrics can both be used in the decision-making algorithm in differential diagnosis of ALN in preoperative period.

**Table 1.** Evaluation of morphological status of axillary lymph nodes

	Non-metastatic (n = 23)	Metastatic (n = 43)	P
Long/short axis	2.42 (1.33-3.80)	1.33 (1.06-2.42)	<.001
Cortical thickness (mm)	2 (2-7)	8 (5-30)	<.001
Long axis	14 (10-25)	16 (10-42)	.058
Fatty hilum, n (%)			
Absent	1 (4.4)	34 (79.1)	<.001
Present	22 (95.6)	9 (20.9)	

Data are presented as median (min-max) except when noted otherwise.

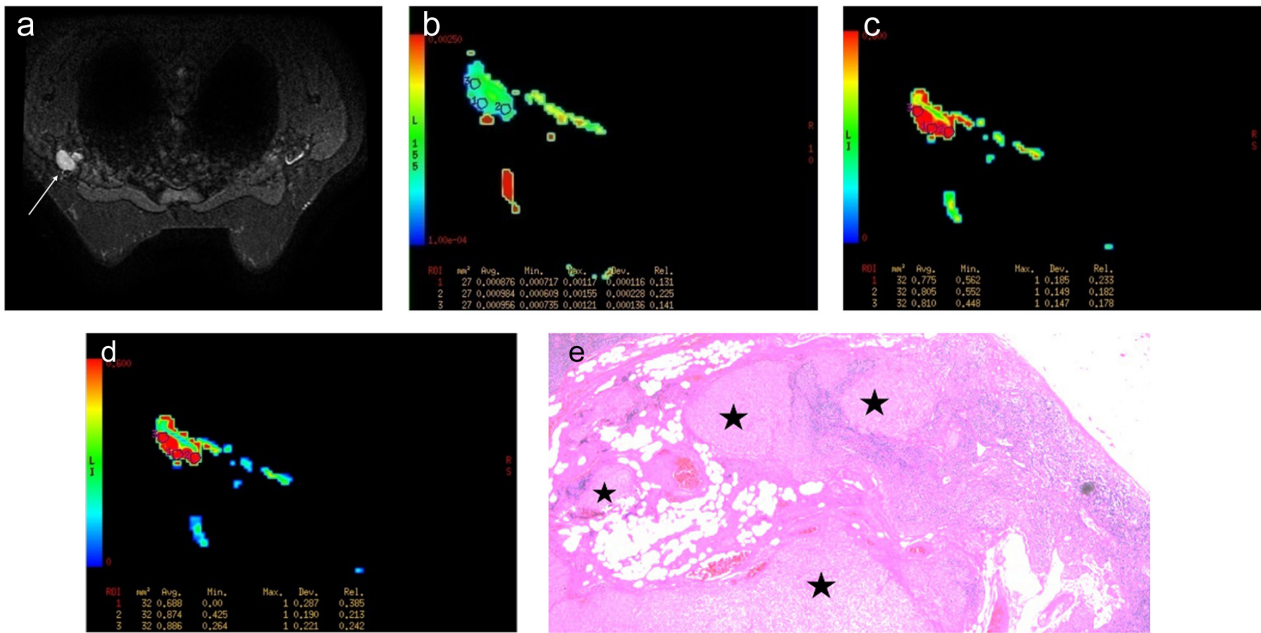


**Figure 1. a-e.** A 39-year-old woman was diagnosed with invasive breast carcinoma NST in the left breast with metastatic ALN. Axial fat-suppressed T2 sequence image (a) shows a lymph node (white arrow) with an increased cortical thickness. Measurements were made by ROI from 3 different parts of the lymph node and the mean was calculated: (b), DWI  $b=800$ , mean ADC  $0.93 \times 10^{-3} \text{ mm}^2/\text{s}$ ; (c), DTI FA  $b=200$ , mean FA 0.80; (d), DTI VA  $b=200$ , mean VA 0.82. H&E staining ( $\times 20$ ) (e) shows axillary lymph node with thick capsule located in fat tissue, light eosinophilic areas below the capsule consisting of high-grade carcinoma metastasis enlarging the lymph node (stars). NST, no special type; ALN, axillary lymph node; ROI, regions of interest, ADC, apparent diffusion coefficient; DTI, diffusion tensor imaging; FA, fractional anisotropy; VA, volume anisotropy; H&E, hematoxylin and eosin.

All images were evaluated by 2 radiologists. The observers were blinded to the patient's information and histopathological information to avoid bias. The consensus was made in cases of disagreement.

#### Histopathological assessment

Surgical pathology records were examined to determine ALN status. Histopathological evaluations were done under a light microscope by 2 pathologists experienced in

breast pathology. Sentinel lymph nodes are determined as tumor negative (non-metastatic) in frozen (intraoperative consultation) and/or paraffin sections. Positive sentinel lymph nodes were further assessed

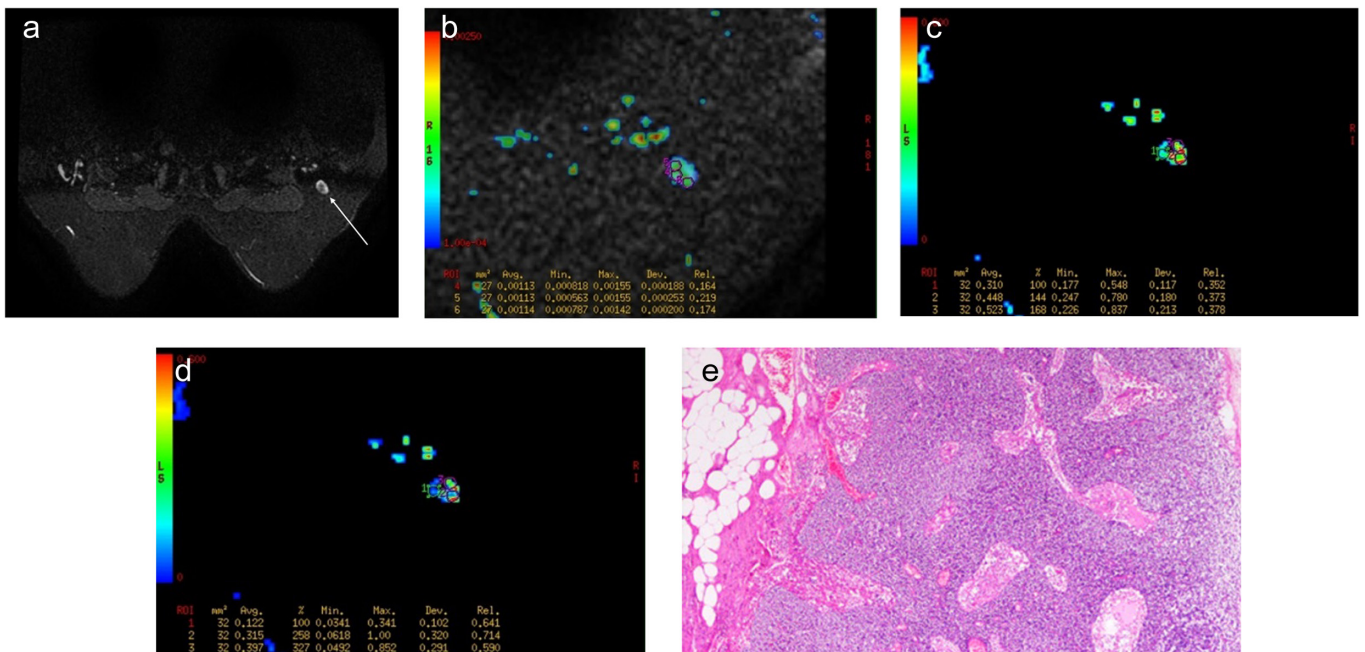


**Figure 2. a-e.** A 47-year-old woman was diagnosed with invasive breast carcinoma NST in the right breast with a reactive sentinel lymph node. Axial fat-suppressed T2 image (a) shows normal lymph node with thin cortex on the right axilla (white arrow). Measurements were made by ROI from 3 different parts of the lymph node and the mean was calculated: (b), DWI  $b=500$ , mean ADC  $1.13 \times 10^{-3} \text{ mm}^2/\text{s}$ ; (c), DTI FA  $b=500$ , mean FA 0.43; (d), DTI VA  $b=200$ , mean VA 0.28. H&E staining ( $\times 40$ ) (e) shows normal axillary lymph node surrounded by fat with expanded sinuses and reactive follicles. NST, no special type; ALN, axillary lymph node; ROI, regions of interest, ADC, apparent diffusion coefficient; DTI, diffusion tensor imaging; FA, fractional anisotropy; VA, volume anisotropy; H&E, hematoxylin and eosin.

as axillary dissections and the largest metastatic lymph node measurements were recorded in final reports.

### Statistical analysis

Statistical evaluation was done using International Business Machines Statistical Package for the Social Sciences software for Windows, Version 21.0. The suitability of the data to the normal distribution was evaluated with the Shapiro–Wilk normality test. A chi-square test was used to evaluate categorical variables. Morphological features, ADC, and FA values were compared using Student’s *t* test when variables showed normal distribution and Mann–Whitney *U* test when variables were not distributed normally. Descriptive analysis of the data was made and non-normalized variables are shown as median (min-max) and normal distributions are shown as mean ± standard deviation. The receiver operating characteristic (ROC) analysis method was used to determine the power of ADC, FA, and VA values in detecting metastasis. Cutoff values were determined using the Youden index. Specificity, sensitivity, negative predictive value (NPV), and positive predictive value (PPV) were calculated. The diagnostic ability to determine lymph node status was also assessed based on the area under the curve (AUC). First, the effect of each factor on lymph node status was assessed by using the univariate logistic regression analysis, and then multivariate logistic regression analysis with enter method was performed to determine the independent variables associated with metastatic ALN, including all of the significant factors from univariate analysis. All tests were 2-tailed and the statistical significance level for *P* value was accepted under .05.

### Results

The median age of a total of 66 women was 48 years (27-76 years). For metastatic and non-metastatic groups, the median age was 50 years (28-71 years) and 47 years (27-76 years), respectively. The time between breast MRI and pathological examination ranged from 0 to 15 days.

In a histopathological evaluation of the malignant breast tumors, 55 (83.4%) were invasive breast carcinoma of no special type and 11 (16.6%) were other types of breast cancer. There were 23 women with negative sentinel lymph node in the non-metastatic group and 43 women with pathologically proven metastasis in the metastatic group.

	Non-metastatic (n=23)	Metastatic (n=43)	<i>P</i>
DWI b=500 ADC	1.02 (1.02-2.12)	1.01 (0.11-2.04)	<.001
DWI b=800 ADC	1.51 (1.01-2.10)	0.94 (0.50-1.97)	<.001
DTI b=200 FA	0.52 ± 0.10	0.65 ± 0.14	<.001
DTI b=500 FA	0.42 ± 0.09	0.59 ± 0.14	<.001
DTI b=200 VA	0.36 ± 0.14	0.52 ± 0.16	<.001
DTI b=500 VA	0.26 ± 0.11	0.46 ± 0.15	<.001

Data are presented as median (min-max) or mean ± standard deviation. ADC values are factors of 10<sup>-3</sup> mm<sup>2</sup>/s. DWI, diffusion-weighted imaging; ADC, apparent diffusion coefficient; DTI, diffusion tensor imaging; FA, fractional anisotropy; VA, volume anisotropy.

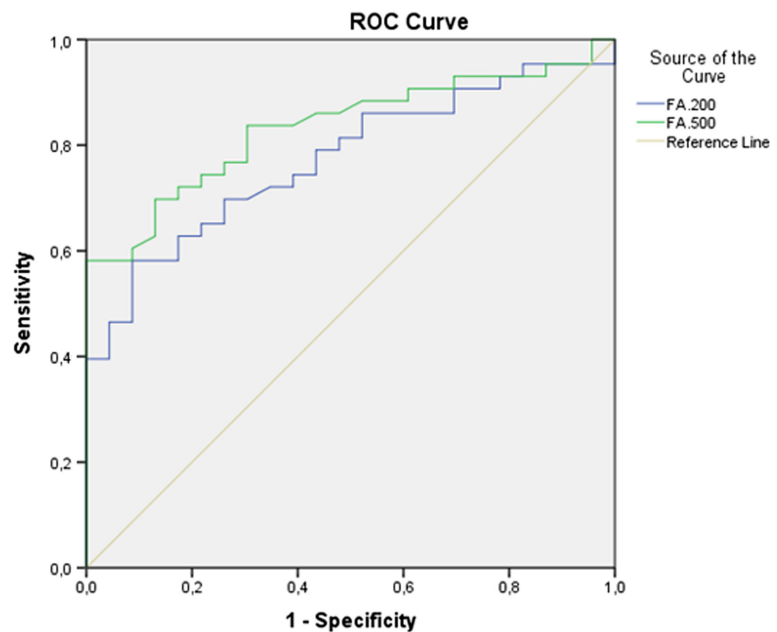


Figure 3. Receiver operating characteristic (ROC) curve analysis of fractional anisotropy.

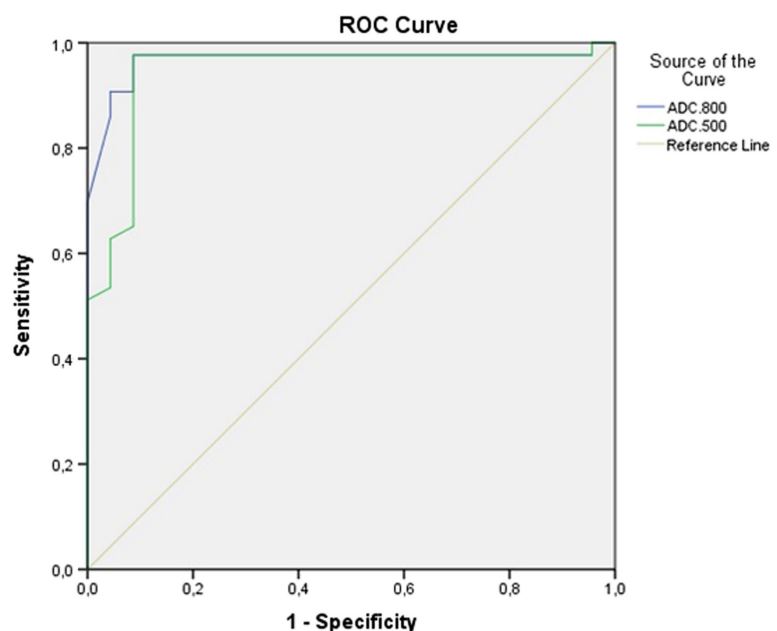


Figure 4. ROC curve analysis of apparent diffusion coefficient.

Among 66 patients, 30 (45.5%) women were in the premenopausal period and 36 (54.5%) women were in the postmenopausal period. Within these patients, 19 women (63.3%) were in the premenopausal period and 24 women (66.7%) in the postmenopausal period had metastatic axillary lymph nodes. There was no statistically significant relationship between ALN involvement and menopausal status ( $P = .777$ ).

Cortical thickness median value was 2 mm (2-7 mm) in non-metastatic ALN and 8 mm (5-30 mm) in metastatic lymph nodes. Cortical thickness of the metastatic ALN was significantly higher than non-metastatic ALN ( $P < .001$ ). Fatty hilum was seen in 95.6% ( $n = 22$ ) non-metastatic ALN although it was only seen in 20.9% of metastatic ALN ( $n = 9$ ). There was a statistically significant difference between ALN status and fatty hilum presence ( $P = .007$ ). The long-axis median value was 14 mm (10-25 mm) in non-metastatic ALN and 16 mm (10-42 mm) in metastatic ALN. There was no statistically significant difference between the long axis and ALN status ( $P = .058$ ). The long-axis-to-short-axis ratio median value was 2.42 (1.33-3.80) in non-metastatic ALN and 1.33 (1.06-2.42) in metastatic ALN. The long-axis-to-short-axis ratio was significantly lower in metastatic ALN when compared to non-metastatic ALN ( $P < .001$ ) (Table 1).

Apparent diffusion coefficient, FA, and VA values were measured in metastatic and non-metastatic ALN (Figures 1 and 2). The DWI  $b = 500$  median value was 1.51 (1.02-2.12) in non-metastatic ALN and 1.01 (0.11-2.04) in metastatic ALN. The DWI  $b = 800$  median value was 1.51 (1.01-2.10) in non-metastatic ALN and 0.94 (0.50-1.97) in metastatic ALN. The DTI  $b = 200$  FA mean value was  $0.52 \pm 0.10$  in non-metastatic ALN and  $0.65 \pm 0.14$  in metastatic ALN. The DTI  $b = 500$  FA mean value was  $0.42 \pm 0.09$  in non-metastatic ALN and  $0.59 \pm 0.14$  in metastatic ALN. The DTI  $b = 200$  VA mean value was  $0.36 \pm 0.14$  in non-metastatic ALN and  $0.52 \pm 0.16$  in metastatic ALN. The DTI  $b = 500$  VA mean value was  $0.26 \pm 0.11$  in non-metastatic ALN and  $0.46 \pm 0.15$  in metastatic ALN (Table 2). Diffusion-weighted imaging  $b = 500$  and  $b = 800$  ADC values of the metastatic ALN were significantly lower than non-metastatic ALN ( $P < .001$  and  $P < .001$ , respectively). However, DTI  $b = 200$  and  $b = 500$  FA values were statistically significantly higher in metastatic

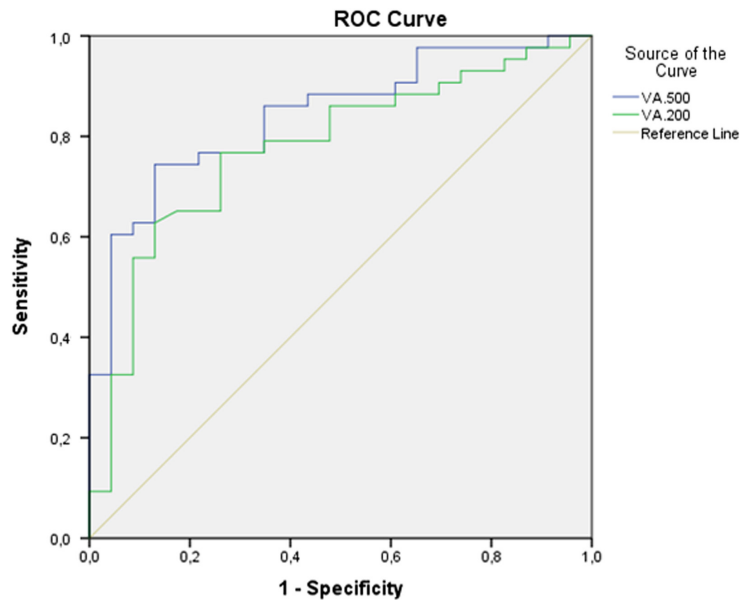


Figure 5. ROC curve analysis of volume anisotropy.

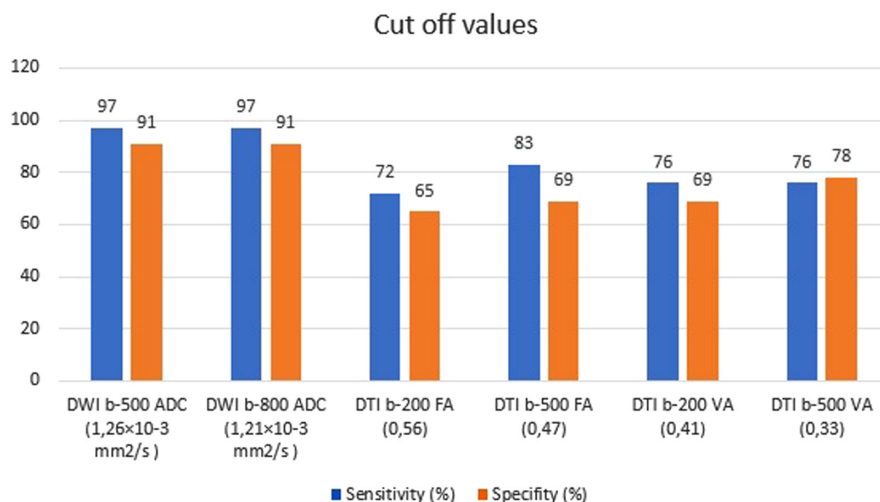


Figure 6. Graphic shows cutoff, sensitivity, and specificity values obtained by ROC curve analysis.

Table 3. Cutoff values for the differentiation of metastatic and non-metastatic lymph nodes						
	Cutoff value	Sensitivity (%)	Specificity (%)	PPV (%)	NPV (%)	AUC
DWI $b = 500$ ADC	$< 1.26$	97.7	91.3	95.5	95.5	$0.94 \pm 0.03$ ( $P < .001$ )
DWI $b = 800$ ADC	$< 1.21$	97.7	91.3	95.5	95.5	$0.96 \pm 0.02$ ( $P < .001$ )
DTI $b = 200$ FA	$> 0.56$	72.1	65.2	76.7	69.6	$0.77 \pm 0.05$ ( $P < .001$ )
DTI $b = 500$ FA	$> 0.47$	83.7	69.6	69.6	83.7	$0.83 \pm 0.04$ ( $P < .001$ )
DTI $b = 200$ VA	$> 0.41$	76.7	69.6	82.5	61.5	$0.77 \pm 0.06$ ( $P < .001$ )
DTI $b = 500$ VA	$> 0.33$	76.7	78.3	86.8	64.3	$0.84 \pm 0.04$ ( $P < .001$ )

ADC values are factors of  $10^{-3} \text{ mm}^2/\text{s}$ .  
DWI, diffusion-weighted imaging; ADC, apparent diffusion coefficient; DTI, diffusion tensor imaging; FA, fractional anisotropy; VA, volume anisotropy; PPV, positive predictive value; NPV, negative predictive value; AUC, area under the curve.

ALN compared to non-metastatic ALN ( $P < .001$  and  $P < .001$ , respectively). Similarly, DTI  $b = 200$  and  $b = 500$  VA values were statistically significantly higher in metastatic ALN compared to non-metastatic ALN ( $P < .001$  and  $P < .001$ , respectively).

**Table 4.** Univariate logistic regression analysis of variables associated with axillary lymph node metastasis

Variable	B	OR	95% CI	P
<b>Morphology</b>				
Long axis	0.11	1.11	0.99-1.26	.058
Long/short axis	-4.59	0.01	0.00-0.08	.001
Cortical thickness	2.53	6.77	2.09-21.9	<.001
Fatty hilum-absent (Ref)	-4.42	83.1	9.8-702.4	<.001
<b>DWI ADC</b>				
b=500	-8.88	0.010	0.00-0.09	<.001
b=800	-8.9	0.010	0.00-0.08	<.001
<b>DTI</b>				
FA b=200	7.41	1660	17.9-15362	<.001
FA b=500	9.62	15061	95.4-237749	<.001
VA b=200	6.56	712	14-35936	<.001
VA b=500	10.14	25352	151.6-423698	<.001

DWI, diffusion-weighted imaging; ADC, apparent diffusion coefficient; DTI, diffusion tensor imaging; FA, fractional anisotropy; VA, volume anisotropy; B, beta; OR, odds ratio.

**Table 5.** Multivariate logistic regression analysis of variables with enter models for predicting axillary lymph node metastasis from morphological features

Variable	B	OR	95% CI	P
Cortical thickness	2.81	16.72	1.15-242.65	.039
Fatty hilum-absent (Ref)	4.07	58.80	0.01-3399.22	.466
Long/short axis	0.99	2.69	0.03-237.37	.665

B, beta; OR, odds ratio.

**Table 6.** Multivariate logistic regression analysis of variables with enter models for predicting axillary lymph node metastasis from DWI

Variable	B	OR	95% CI	P
DWI ADC b=500	1.26	3.53	0.04-306.01	.580
DWI ADC b=800	-10.09	0.001	0.001-0.01	.001

DWI, diffusion-weighted imaging; ADC, apparent diffusion coefficient; B, beta; OR, odds ratio.

**Table 7.** Multivariate logistic regression analysis of variables with enter models for predicting axillary lymph node metastasis from DTI

Variable	B	OR	95% CI	P
DTI FA b=200	1.05	2.85	0.001-53194.7	.835
DTI FA b=500	2.14	8.48	0.003-27086.9	.603
DTI VA b=200	1.49	4.43	0.003-7766.3	.696
DTI VA b=500	7.64	2081	1.7-24102.8	.034

DTI, diffusion tensor imaging; FA, fractional anisotropy; VA, volume anisotropy; B, beta; OR, odds ratio.

Based on the ROC curves, the diagnostic performance of the DWI and DTI parameters with cutoff values for the differentiation of non-metastatic and metastatic ALN were measured (Figures 3-6). A cutoff value of  $1.26 \times 10^{-3} \text{ mm}^2/\text{s}$  for b=500 ADC and  $1.21 \times 10^{-3} \text{ mm}^2/\text{s}$  for b=800 ADC had 97.7%

sensitivity and 91.3% specificity. In these cutoff values, there were 2 false-positive and 1 false-negative cases for b=500 and b=800 DWI, respectively, and the PPV and NPV for the 2 measurements were 95.5%. A cutoff value of 0.56 for b=200 FA resulted in 8 false-positive and 12 false-negative

cases with 72.1% sensitivity, 65.2% specificity, 76.7% PPV, and 69.6% NPV. A cutoff value of 0.47 for b=500 FA resulted in 7 false-positive and 7 false-negative cases with 83.7% sensitivity, 69.6% specificity, 69.6% PPV, and 83.7% NPV. A cutoff value of 0.41 for b=200 VA resulted in 10 false-positive and 7 false-negative cases with 76.7% sensitivity, 69.6% specificity, 82.5% PPV, and 61.5% NPV. A cutoff value of 0.33 for b=500 VA resulted in 10 false-positive and 5 false-negative cases with 76.7% sensitivity, 78.3% specificity, 86.8% PPV, and 64.3% NPV (Table 3).

The risk of metastatic ALN status associated with each morphologic, DWI, and DTI parameters was evaluated by univariate logistic regression (Table 4). There were significant differences between cortical thickness, hilum presence, long-axis-to-short-axis ratio, DWI and DTI parameters, and ALN status. However, the long axis showed no significant association with ALN status on univariate analysis ( $P = .058$ ). Those variables which showed statistics significance on univariate analysis were used for the multivariate logistic regression analysis.

On multivariate analysis, cortical thickness was found to be independent predictors for metastatic ALN status from morphological features (Table 5). Also, ADC b=800 was found to be independent predictors for metastatic ALN status from DWI (Table 6) and VA 500 was found to be independent predictors for metastatic ALN status from DTI (Table 7). In the comparison of the most important factors of morphological, DWI, and DTI parameters in logistic regression analysis with enter model, ADC b=800 was maintained independently in predicting metastatic ALN (Table 8). In addition, when ADC b=800, cortical thickness, and VA b=500 parameters are used together to detect metastatic ALN, the specificity and sensitivity were 95.7% and 100% respectively. PPV was 100% and NPV was 97.7%.

## Discussion

Axillary lymph node is considered to be the most significant prognostic factor in the clinical management of breast cancer patients.<sup>20</sup> Image-based methods for detecting ALN metastasis is an active research area to prevent unnecessary axillary dissection. Although the morphological features of the ALNs can be better

**Table 8.** Multivariate logistic regression analysis of variables with enter models for predicting axillary lymph node metastasis

Variable	B	OR	95% CI	P
Cortical thickness	2.51	6.65	0.57-77.11	.121
DWI ADC b=800	-6.15	0.001	0.00-3.5	.042
DTI VA b=500	4.21	29577	0.10-3744810	.331

DWI, diffusion-weighted imaging; ADC, apparent diffusion coefficient; DTI, diffusion tensor imaging; VA, volume anisotropy; B, beta; OR, odds ratio.

visualized in US, there are some features to identify metastatic lymph nodes like loss of hilum, irregular edges, and irregular cortical thickness in MRI.<sup>4</sup> Mortorello et al.<sup>21</sup> reported a statistically significant correlation between metastatic ALN and the absence of fatty hilum in contrast-enhanced MRI.<sup>21</sup> Similarly, our study found a statistically significant correlation between the absence of fatty hilum and metastatic lymph nodes. Kim et al.<sup>22</sup> found that all cortical thickness parameters showed significant association with nodal metastases in both US and MRI. In the same study, they reported the long-axis-to-short-axis ratio in MRI was not significantly associated with nodal metastases.<sup>22</sup> In our study, cortical thickness and long-axis ratio in MRI were significantly associated with ALN metastasis, and cortical thickness was found to be one of the most important morphological parameters.

Extracellular random motion of water molecules together with isotropic diffusion rate is quantified with ADC value in DWI. Diffusion-weighted imaging can also provide information about microenvironments such as perfusion, flow effects, intracellular macromolecules, and extracellular matrix volume.<sup>23,24</sup> In diffusion restricted by surrounding cells or basement membranes, diffusion toward certain directions increases more. In this way, diffusion is fast and anisotropic in limited directions. Fractional anisotropy value shows the ratio of the anisotropic part of the diffusion to the whole diffusion in the tissue. Diffusion restriction in surrounding tissues in the presence of malignancy causes a change in anisotropic motion.<sup>25</sup>

The results of this study suggest that metastatic ALN showed significantly higher FA values and lower ADC values. Diffusion-weighted imaging b=800 ADC was the most discriminative variable for predicting metastatic lymph nodes (AUC:  $0.96 \pm 0.02$ ; cutoff value  $1.21 \times 10^{-3} \text{ mm}^2/\text{s}$ ).

In a meta-analysis consisting of 13 studies by Xing et al.,<sup>12</sup> ADC value of metastatic

ALN was found to be statistically significantly lower than non-metastatic ALN.<sup>12</sup> However, in recent studies, there are conflicting data on ADC value in ALN status. Atallah et al.<sup>26</sup> revealed that in breast cancer patients, the difference in ADC values between ipsilateral and contralateral lymph nodes is not significantly associated with ALN positivity and Ramírez-Galván et al.<sup>27</sup> stated that the ADC value of metastatic ALN was significantly higher than non-metastatic ALN in 44 cases. In line with the previous meta-analysis study, our study showed that metastatic ALN had lower mean ADC values than non-metastatic ALN and the difference was statistically significant.

Studies are emerging in terms of DTI and FA in the evaluation of breast cancer to enable optimal patient management.<sup>13,14,22</sup> Cakir et al.<sup>13</sup> examined ADC and FA in malignant and benign breast lesions in 55 patients. They reported that FA was not discriminative for benign and malignant lesions. In another study, Jiang et al.<sup>14</sup> reported in their study that FA value was found to be statistically significantly higher in malignant mass compared to benign mass. In line with this study, we found that FA and VA values were significantly higher in metastatic ALN compared to non-metastatic ALN.

In a study of 99 patients, Chayakulkeeree et al.<sup>28</sup> found the sensitivity of breast MRI for detecting metastatic ALN to be 98.5%, the NPV to be 96.4%, specificity to be 57.8%, and the PPV to be 71%.<sup>28</sup> In our study, the specificity and PPV of MRI, in which ADC, FA, and morphological features were evaluated together, detecting ALN status were 95.7% and 100% respectively, while its sensitivity and NPV were 100% and 97.7%. These results show that useful information may be gained on the axilla in patients undergoing breast MRI.

The relatively low number of patients and the usage of conventional ROI-based technique for quantifying the diffusion tensor image were limitations of our study. Further

larger prospective studies are needed to validate the clinical usefulness of our research.

In conclusion, we evaluated the contribution of FA and ADC values obtained from DTI and DWI in determining the status of the ALN in breast cancer patients. Metastatic ALN had a significantly lower ADC value than non-metastatic ALN, and FA values of metastatic ALN were found to be significantly higher than non-metastatic ALN. Also, ADC value had a better diagnostic performance than morphological features and FA. Based on the results of this study, we believe that DWI and DTI may contribute to differentiating metastatic ALN from non-metastatic ALN in a preoperative setting.

### Conflict of interest disclosure

The authors declared no conflicts of interest.

### References

1. Bray F, Ferlay J, Soerjomataram I, Siegel RL, Torre LA, Jemal A. Global cancer statistics 2018: GLOBOCAN estimates of incidence and mortality worldwide for 36 cancers in 185 countries. *CA Cancer J Clin.* 2018;68(6):394-424. [\[CrossRef\]](#)
2. Kuhl CK. The changing world of breast cancer: a radiologist's perspective. *Invest Radiol.* 2015;50(9):615-628. [\[CrossRef\]](#)
3. Choi HY, Park M, Seo M, Song E, Shin SY, Sohn YM. Preoperative axillary lymph node evaluation in breast cancer: current issues and literature review. *Ultrasound Q.* 2017;33(1):6-14. [\[CrossRef\]](#)
4. Maxwell F, de Margerie Mellon C, Bricout M, et al. Diagnostic strategy for the assessment of axillary lymph node status in breast cancer. *Diagn Interv Imaging.* 2015;96(10):1089-1101. [\[CrossRef\]](#)
5. Marino MA, Avendano D, Zapata P, Riedl CC, Pinker K. Lymph node imaging in patients with primary breast cancer: concurrent diagnostic tools. *Oncologist.* 2020;25(2):e231-e242. [\[CrossRef\]](#)
6. Hafiz A, Adeniji-Sofoluwe AT, Ademola AF, Obajimi MO. Sonographic evaluation of axillary lymph nodes in women with newly diagnosed breast cancer at the university college hospital Ibadan, Nigeria. *Niger Postgrad Med J.* 2018;25(2):79-86. [\[CrossRef\]](#)
7. Peters NH, Borel Rinkes IH, Zuithoff NP, Mali WP, Moons KG, Peeters PH. Meta-analysis of MR imaging in the diagnosis of breast lesions. *Radiology.* 2008;246(1):116-124. [\[CrossRef\]](#)
8. Runge VM. Safety of approved MR contrast media for intravenous injection. *J Magn Reson Imaging.* 2000;12(2):205-213. [\[CrossRef\]](#)
9. Onaygil C, Kaya H, Ugurlu MU, Aribal E. Diagnostic performance of diffusion tensor imaging parameters in breast cancer and correlation with the prognostic factors. *J Magn Reson Imaging.* 2017;45(3):660-672. [\[CrossRef\]](#)

10. Woodhams R, Ramadan S, Stanwell P, et al. Diffusion-weighted imaging of the breast: principles and clinical applications. *RadioGraphics*. 2011;31(4):1059-1084. [\[CrossRef\]](#)
11. Elmesidy DS, Badawy EAMO, Kamal RM, Khalaf ESE, AbdelRahman RW. The additive role of diffusion-weighted magnetic resonance imaging to axillary nodal status evaluation in cases of newly diagnosed breast cancer. *Egypt J Rad Nucl Med*. 2021;52:1-12.
12. Xing H, Song CL, Li WJ. Meta analysis of lymph node metastasis of breast cancer patients: clinical value of DWI and ADC value. *Eur J Radiol*. 2016;85(6):1132-1137. [\[CrossRef\]](#)
13. Yamaguchi K, Schacht D, Nakazono T, Irie H, Abe H. Diffusion weighted images of metastatic as compared with nonmetastatic axillary lymph nodes in patients with newly diagnosed breast cancer. *J Magn Reson Imaging*. 2015; 42(3):771-778. [\[CrossRef\]](#)
14. Partridge SC, Ziadloo A, Murthy R, et al. Diffusion tensor MRI: preliminary anisotropy measures and mapping of breast tumors. *J Magn Reson Imaging*. 2010;31(2):339-347. [\[CrossRef\]](#)
15. Roberts TP, Schwartz ES. Principles and implementation of diffusion-weighted and diffusion tensor imaging. *Pediatr Radiol*. 2007;37(8):739-748. [\[CrossRef\]](#)
16. Cakir O, Arslan A, Inan N, et al. Comparison of the diagnostic performances of diffusion parameters in diffusion weighted imaging and diffusion tensor imaging of breast lesions. *Eur J Radiol*. 2013;82(12):e801-e806. [\[CrossRef\]](#)
17. Jiang R, Ma Z, Dong H, Sun S, Zeng X, Li X. Diffusion tensor imaging of breast lesions: evaluation of apparent diffusion coefficient and fractional anisotropy and tissue cellularity. *Br J Radiol*. 2016;89(1064):20160076. [\[CrossRef\]](#)
18. Arslan G, Altintoprak KM, Yirgin IK, Atasoy MM, Celik L. Diagnostic accuracy of metastatic axillary lymph nodes in breast MRI. *Springerplus*. 2016;5(1):735. [\[CrossRef\]](#)
19. Baltzer PA, Dietzel M, Burmeister HP, et al. Application of MR mammography beyond local staging: is there a potential to accurately assess axillary lymph nodes? Evaluation of an extended protocol in an initial prospective study. *Am J Roentgenol*. 2011;196(5):W641-W647. [\[CrossRef\]](#)
20. Carter CL, Allen C, Henson DE. Relation of tumor size, lymph node status, and survival in 24,740 breast cancer cases. *Cancer*. 1989;63(1): 181-187. [\[CrossRef\]](#)
21. Mortellaro VE, Marshall J, Singer L, et al. Magnetic resonance imaging for axillary staging in patients with breast cancer. *J Magn Reson Imaging*. 2009;30(2):309-312. [\[CrossRef\]](#)
22. Kim WH, Kim HJ, Lee SM, et al. Preoperative axillary nodal staging with ultrasound and magnetic resonance imaging: predictive values of quantitative and semantic features. *Br J Radiol*. 2018;91(1092):20180507. [\[CrossRef\]](#)
23. Kim JK, Kim KA, Park BW, Kim N, Cho KS. Feasibility of diffusion-weighted imaging in the differentiation of metastatic from nonmetastatic lymph nodes: early experience. *J Magn Reson Imaging*. 2008;28(3):714-719. [\[CrossRef\]](#)
24. Meyer HJ, Garnov N, Surov A. Comparison of two mathematical models of cellularity calculation. *Transl Oncol*. 2018;11(2):307-310. [\[CrossRef\]](#)
25. Nissan N, Furman-Haran E, Feinberg-Shapiro M, et al. Tracking the mammary architectural features and detecting breast cancer with magnetic resonance diffusion tensor imaging. *J Vis Exp*. 2014;94:e52048.
26. Atallah D, Moubarak M, Arab W, El Kassis N, Chahine G, Salem C. MRI-based predictive factors of axillary lymph node status in breast cancer. *Breast J*. 2020;26(11):2177-2182. [\[CrossRef\]](#)
27. Ramírez-Galván YA, Cardona-Huerta S, Elizondo-Riojas G, Álvarez-Villalobos NA, Campos-Coy MA, Ferrara-Chapa CM. Does axillary lymph node size predict better metastatic involvement than apparent diffusion coefficient (ADC) value in women with newly diagnosed breast cancer? *Acta Radiol*. 2020;61(11): 1494-1504. [\[CrossRef\]](#)
28. Chayakulkheeree J, Pungrassami D, Prueksadee J. Performance of breast magnetic resonance imaging in axillary nodal staging in newly diagnosed breast cancer patients. *Pol J Radiol*. 2019;84:e413-e418. [\[CrossRef\]](#)